Letters

Wireless Power and Data Transfer System Using Multidirectional Magnetic Coupler for Swarm AUVs

Yingqin Zeng, Conghui Lu, Renzhe Liu, Xiangrui He, Cancan Rong, *Member, IEEE*, and Minghai Liu

***Abstract*—In this letter, a simultaneous wireless power and data transfer system based on a novel multidirectional magnetic coupler is presented for the application of swarm AUVs. The transmitting coil consisting of two reversely wound helix loops can generate a multidirectional magnetic field in space, which supplies power to multiple arc-shaped receiving coils placed in different directions. Aiming at high coupling strength and low core volume, a multi-objective genetic algorithm is used to optimize coil parameters. In addition, a hybrid injection communication method based on *LCC-S* compensation topology is proposed and analyzed. An experiment platform is built and the results show that the system can achieve 92.25% efficiency at a power level of 200 W when four AUVs are powered. Meanwhile, the transferred data are successfully recovered at the data rate of 30 kbps.**

***Index Terms*—Autonomous underwater vehicles (AUVs), data transfer, magnetic coupler, multiple loads, wireless power transfer (WPT).**

I. Introduction

Wireless power transfer (WPT) is considered an outstanding underwater energy supply scheme, which can significantly improve the endurance and concealment of autonomous underwater vehicle (AUV) [1], [2]. With the ever-increasing demands for marine resource exploration, the single AUV has been facing the restrictions of a small operating range, poor work ability, and low redundancy. The cooperative work of swarm AUVs provides an excellent way to accomplish difficult tasks. Therefore, the multiload WPT technology is a promising approach to charging AUVs.

Manuscript received 2 August 2022; revised 6 September 2022 and 2 October 2022; accepted 6 October 2022. Date of publication 13 October 2022; date of current version 18 November 2022. This work was supported by State Key Laboratory of Advanced Electromagnetic Engineering and Technology under Grant AEET 2022KF007. *(Corresponding author: Minghai Liu.)*

Yingqin Zeng, Renzhe Liu, Xiangrui He, and Minghai Liu are with the School of Electrical and Electronic Engineering, Huazhong University of Science and Technology, Wuhan 430074, China (e-mail: yqzeng@hust.edu.cn; liurenzhe@hust.edu.cn; xiangruihe@hust.edu.cn; mhliu@hust.edu.cn).

Conghui Lu is with the China North Vehicle Research Institute, Beijing 100072, China (e-mail: luchw3@163.com).

Cancan Rong is with the School of Electrical and Power Engineering, China University of Mining and Technology, Xuzhou 221116, China (e-mail: ccrong@cumt.edu.cn).

Color versions of one or more figures in this article are available at https://doi.org/10.1109/TPEL.2022.3214318.

Digital Object Identifier 10.1109/TPEL.2022.3214318

According to the transmission mode of the WPT system, the multiload magnetic couplers can be classified into the directional structure and the multidirectional structure. In [3], the directional magnetic coupler in a domino form can wirelessly supply power to multiple loads distributed over a long distance. In order to expand the positional freedom of WPT system, the dual-band three-dimensional (3D) circular and square transmitting (Tx) coils were proposed in [4], allowing power to the receiving (Rx) coils located at different positions. Nevertheless, Rx coils with different frequencies cannot receive power at the same time. A three-phase WPT system based on *LCC-S* topology is designed in [5], which can achieve the power stability of multiple loads. However, this technique needs multiple-phase voltage regulation, which is complex and expensive in practice. In [6], a cylindrical Tx coil without any active control was presented with the ability to provide a homogeneous magnetic field for the surrounding Rx coils. Nevertheless, this work only optimizes the Tx coil using a parametric sweep. The above research is related to air applications. Recently, there have been a few studies on multi-load WPT systems for underwater applications. Although a segmented arc solenoid Tx coil capable of charging multiple AUVs has been designed in [7], the Rx structure is not compatible with the cylindrical hull of an AUV. Moreover, the structure is sensitive to Rx coil misalignment. Thus, designing a high-performance magnetic coupler for swarm AUVs combined with an efficient optimization method is still an unsolved challenge.

During power delivery, the introduction of data communication to accomplish closed-loop control improves the reliability and safety of the system. Currently, power and data transfer modes using the same coupling channel via an independent data carrier have shown great potential. In [8] and [9], power and data are transmitted at different moments by controlling switching devices, namely the time-sharing multiplexing method. But this communication approach will inevitably lead to a large output power fluctuation. In [10] and [11], a simultaneous wireless power and data transfer (SWPDT) system is presented, in which the high-frequency coupled transformers are used for data carrier injection and extraction. However, this method has a high power loss of the data signal during transmission. In [12], a novel data injection method was developed based on the structural characteristics of the double-D coil to achieve power lossless data

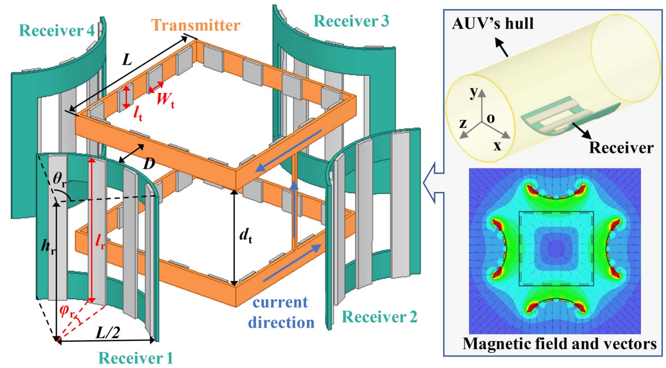

Fig. 1. General overview of the multidirectional WPT system for swarm AUVs.

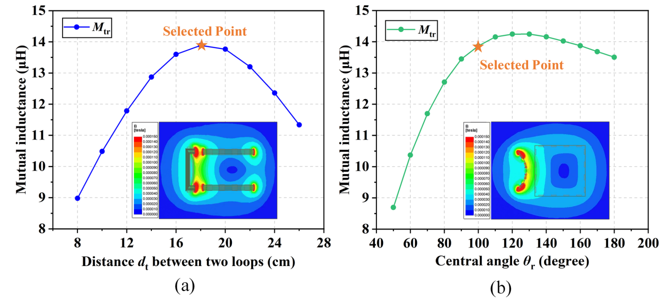

Fig. 2. Mutual inductance versus coil parameters. (a) Distance d_{tr} between two loops. (b) Central angle θ_r.

transfer. Nevertheless, this approach has limited applicability due to the special coil structure.

For the abovementioned analysis, this letter proposes a well-designed and high-efficiency SWPDT system for multiple AUVs. The multidirectional magnetic coupler is designed and optimized with a comprehensive consideration of compatibility with the AUV's hull, transfer performance, and weight. Then the simultaneous transfer mode of signal and power has been fully studied. Finally, a SWPDT prototype has been established to verify the studies. The main contributions to this letter are as follows:

1) A cube-shaped Tx coil and an arc-shaped Rx coil with equally spaced ferrite cores are proposed for swarm AUV charging. The parameters of Tx and Rx coils are determined by adopting a multiobjective genetic algorithm, which can achieve high mutual inductance and low core volume.
2) A hybrid injection communication method that utilizes partial Rx coil, Tx coil, and an additional transformer to transmit data is presented, which is compatible with different magnetic coupler structures.

II. Magnetic Coupler Design

The general overview of the multidirectional WPT system for swarm AUVs is depicted in Fig. 1. On the Rx part, the arc-shaped structure is applied to match the AUV's curly hull. The Tx coil consists of two reversely wound helix loops. In order to determine the geometrical shape of the Tx coil, square and circular Tx coils with the same design parameters are analyzed. Specifically, both coils have an identical turn number, turn spacing, and distance between two loops, and the side length of a square coil is equal to the diameter of a circular coil. The mutual inductance between the square Tx coil and the arc-shaped Rx coil is higher compared with the circular Tx coil at a fixed transfer distance of D. Hence, the square helix loops are used for better transfer performance. The currents of two loops powered by a single source are in opposite directions, guaranteeing a multidirectional magnetic field surrounding the Tx coil. Therefore, the power can be transmitted to multiple Rx coils arranged around the Tx coil. Based on the magnetic field distribution characteristics, ferrite cores with lateral uniform distribution are adopted to effectively enhance the coupling and reduce leakage magnetic fields. According to the size restrictions and docking requirements of the AUVs, the loop dimension L of coils is 30 cm with a height h_r of 25 cm, while the gap D of Tx and Rx coils is 5 cm. The turn number of each helix loop in the Tx coil is set at 9, and the turn number of the Rx coil is set at 13. In order to optimize the two key coil parameters, that is, distance d_t between two loops and central angle θ_r, the influence of the above parameters on mutual inductance M_{tr} is investigated one by one when other coil parameters are fixed, as demonstrated in Fig. 2. The $d_t = 18$ cm and $\theta_r = 100°$ are selected for the design, which satisfies strong coupling ability and low coupler volume.

It is well known that the mutual inductance will be increased by inserting Mn–Zn ferrite material as a core in the magnetic coupler [13]. However, a larger core volume leads to higher weight and cost. Therefore, it is necessary to optimize the ferrite core size so that the core volume is reduced while still ensuring an acceptable mutual inductance. We built it as a mathematical model of the multiobjective optimization problem. The objective functions can be described as follows.

$$\begin{cases} \text{Minimize } V_t = f_1(l_t, W_t) \\ \text{Minimize } V_r = f_2(l_r, \varphi_r) \\ \text{Minimize } -M_{tr} = f_3(l_t, W_t, l_r, \varphi_r) \end{cases} \tag{1}$$

V_t and V_r indicate the ferrite core volume of the Tx and Rx coils, respectively. When the core thickness is fixed at 5 mm, M_{tr}, V_t, and V_r are dependent on the core length l_t and width W_t in Tx coil, and the core length l_r and radian φ_r in Rx coil. The optimization constraints are that the ferrite core should not overlap and its length cannot exceed a certain value, as illustrated in (2).

$$\begin{cases} 1.5\,\text{cm} \le l_t \le 5.5\,\text{cm} \\ 1.5\,\text{cm} \le W_t \le 5.5\,\text{cm} \\ 15\,\text{cm} \le l_r \le 27.5\,\text{cm} \\ 5° \le \varphi_r \le 25° \end{cases} \tag{2}$$

The Nondominant Sorting Genetic Algorithm II (NSGA-II) is an excellent algorithm for solving multiobjective optimization problems due to the reduction of computational complexity, the introduction of elite strategy, and the guarantee of population diversity [14], [15]. The optimization flowchart of the magnetic coupler using NSGA-II in Maxwell and MATLAB cosimulation

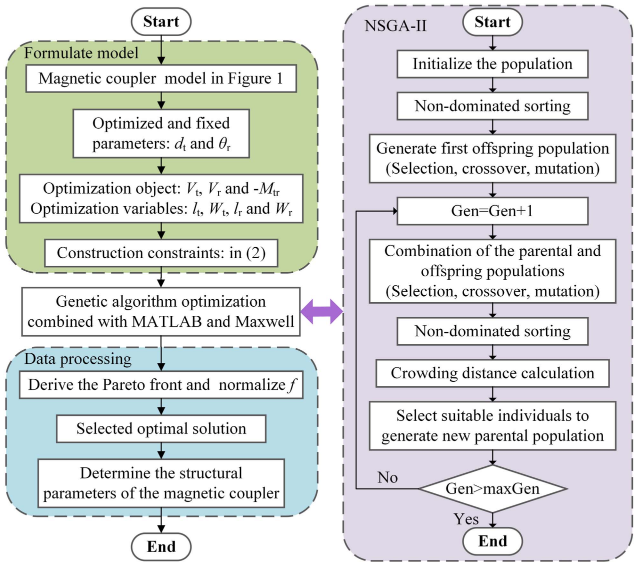

Fig. 3. Flowchart for optimizing the magnetic coupler.

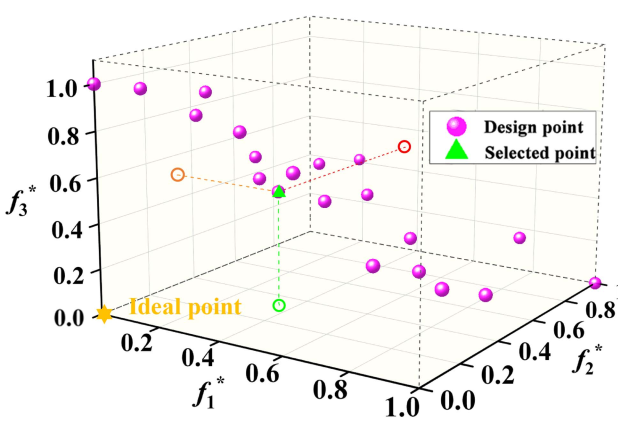

Fig. 4. Pareto front for the magnetic coupler optimization.

environments is shown in Fig. 3. The main program of NSGA-II is written in MATLAB. First, the design variables generated by NSGA-II are passed to the simulation model of ANSYS Maxwell. Then, ANSYS Maxwell builds the corresponding 3-D finite element model and passes the simulated mutual inductance to MATLAB to obtain the objective function value. The obtained Pareto front is plotted in Fig. 4, where the objective variables are normalized by adopting min–max normalization.

$$f^* = \frac{f - f_{\min}}{f_{\max} - f_{\min}} \tag{3}$$

The structure with $f_1{}^* = f_2{}^* = f_3{}^* = 0$ is the ideal design, but no such structure exists. The marked point with $l_\mathrm{t} = 3.5$ cm, $W_\mathrm{t} = 3.5$ cm, $l_\mathrm{r} = 27.5$ cm, and $\varphi_\mathrm{r} = 10°$ is chosen as the optimal design, which realizes a great tradeoff between M_tr, V_t, and V_r and has the closest distance to the ideal point.

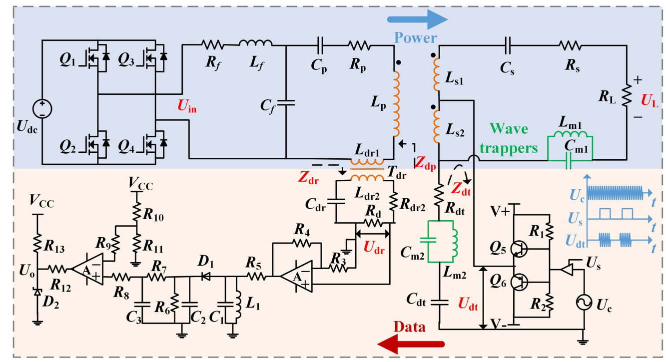

Fig. 5. Schematic circuit of the SWPDT system.

III. Equivalent Circuit Analysis of SWPDT System

The schematic circuit of the SWPDT system is depicted in Fig. 5. An *LCC-S* compensation topology is employed on the power transfer link to ensure the constant-voltage output under varying load numbers. The data signal is injected into the partial Rx coil and coupled to the data receiver via the Tx coil and transformer T_dr. The wave trapper on the power receiver side resonates at data transfer frequency, and the wave trapper on the data transmitter side resonates at power transfer frequency, thus suppressing crosstalk interference. A simple and convenient on–off keying modulation scheme is applied to transmit data. U_c, U_s, and U_dt represent the high-frequency carrier wave, original data, and modulated data respectively. In the study, the operating frequencies of the power and data carrier were set at 249 kHz and 1.5 MHz separately.

A. Analysis on Power Transfer Channel

On the primary side, there are four components, namely the Tx inductor L_p, series capacitor C_p, parallel capacitor C_f and compensation inductor L_f, constituting an *LCC* resonant circuit. On the secondary side, the Rx inductor L_s and compensation capacitor C_s are connected in series. M_tr denotes the mutual inductance between the Tx and Rx coils. In order to realize constant Tx current and load-independent output voltage, the system parameters need to be satisfied

$$\begin{cases} j\omega_p L_f + 1/(j\omega_p C_f) = 0 \\ j\omega_p L_p + 1/(j\omega_p C_p) + 1/(j\omega_p C_f) = 0 \\ j\omega_p L_s + 1/(j\omega_p C_s) = 0 \end{cases} \tag{4}$$

When neglecting the parasitic resistances of coils, the current flowing through Tx coil and output voltage can be written as

$$\begin{cases} \dot{I}_P = \dot{U}_{in}/(j\omega_p L_f) \\ \dot{U}_L = M_{tr}\dot{U}_{in}/L_f \end{cases} \tag{5}$$

The received power for each load is calculated as

$$P_{out} = M_{tr}^2 U_{in}^2/(L_f^2 R_L) \tag{6}$$

B. Analysis on Data Transfer Channel

During data transfer, the branch of the inductor $L_{\mathrm{s}1}$ is regarded as an open circuit because the wave trapper at the secondary side

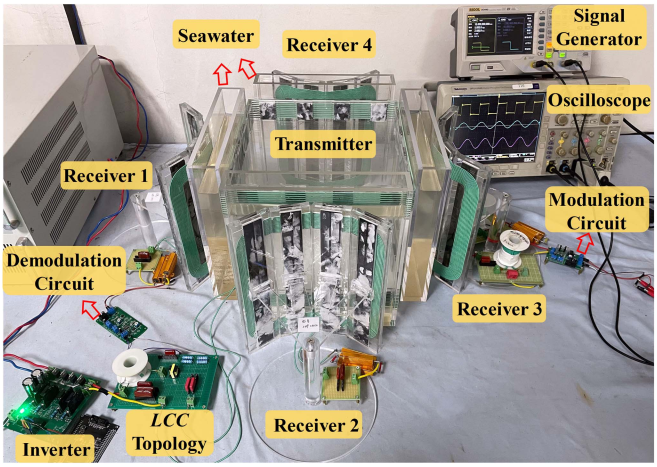

Fig. 6. Experimental prototype of the SWPDT system.

can block the high-frequency wave. The branch of the capacitor C_f can be considered a short circuit due to its low-impedance state at data transfer frequency f_{d}. The compensation capacitors C_{dt} and C_{dr} are selected to match the data transmitter and receiver network at f_{d}, respectively. The mathematical relation can be expressed as

$$\begin{cases} j\omega_d L_{dr2} + 1/(j\omega_d C_{dr}) = 0 \\ j\omega_d L_{s2} + 1/(j\omega_d C_{dt}) + j\omega_d L_{m2}/(1-\omega_d^2 L_{m2} C_{m2}) = 0 \end{cases} \tag{7}$$

The loop impedances of the data receiver, primary side, and data transmitter could be derived as

$$\begin{cases} Z_{dr} = R_{dr2} + R_d \\ Z_{dp} = R_p + j\omega_d(L_p + L_{dr1}) + (\omega_d M_r)^2/Z_{dr} \\ Z_{dt} = R_{dt} + (\omega_d M_{tr2})^2/Z_{dp} \end{cases} \tag{8}$$

where M_{r} is the mutual inductance of the coupled transformer T_{dr} and M_{tr2} is the mutual inductance between the Tx coil and partial Rx coil. So the data gain could be deduced

$$\frac{U_{dr}}{U_{dt}} = \frac{R_d}{Z_{dr}} \frac{j\omega_d M_r}{Z_{dp}} \frac{j\omega_d M_{tr2}}{Z_{dt}} \tag{9}$$

The received data voltage U_{dr} is extracted from the resistance R_{dr}. Then, the wave is processed by the signal demodulation circuit to obtain output data U_{o}.

IV. Experimental Verification

An experimental prototype of the SWPDT system based on the proposed multidirectional magnetic coupler has been established, as shown in Fig.6. Considering the practical ferrite specification and fabrication technique, a 2 × 3 square ferrite array is substituted for each arc-shaped ferrite block row of the Rx coil. The dimensions of the square ferrite cell are 90 × 15 × 5 mm. A double-layer 2 × 2 array structure is utilized in the ferrite material of the Tx coil, where the dimension of the ferrite cell is 17.6 × 15.6 ×2.2 mm. Four tanks filled with seawater are placed around the Tx coil to simulate marine environment. The conductivity and relative permittivity of seawater are 3.3 S/m and 81, respectively. The electrical parameters of the experimental

TABLE I
Electrical Parameters of Experimental Setup

Tx coil		Rx coil		Communication part	
Symbol	Value	Symbol	Value	Symbol	Value
L_{p}	135.6 μH	L_{s}	112.5 μH	C_{dt}	1.07nF
L_{f}	19.7 μH	L_{s1}	72.7 μH	L_{dr1}	13.5 μH
C_{f}	20.97nF	L_{s2}	8.14 μH	L_{dr2}	13.5 μH
C_{p}	3.13nF	C_{s}	2.97nF	C_{dr}	787pF
M_{tr}	13.65 μH	M_{tr2}	3.2 μH	R_{d}	10 Ω
f_{p}	249.2 kHz	R_{L}	25 Ω	f_{d}	1.5 MHz

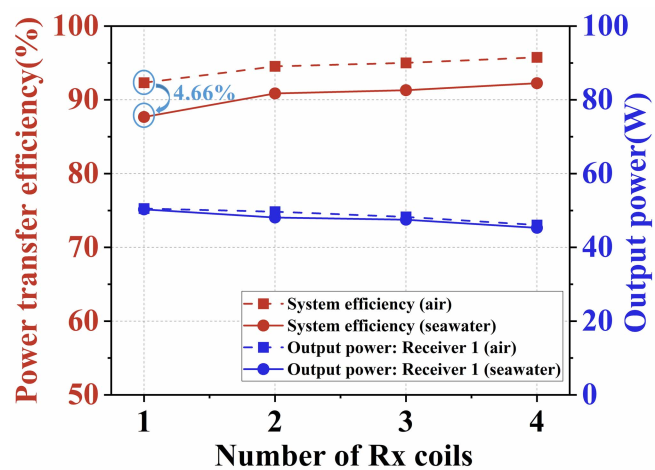

Fig. 7. PTE and output power versus number of Rx coils.

setup are tabulated in Table I. In the experiment, the input dc voltage U_{dc} is fixed at 58 V, and the transfer distance is set to 5 cm.

For various numbers of Rx coils, the total power transfer efficiency (PTE) and output power of either receiver are measured, as shown in Fig. 7. Each Rx coil has essentially the same circuit parameters. It can be found that the PTE is reduced by 4.66% at most and the output power remains basically unchanged from air to seawater. As the number of Rx coils varies from 1 to 4, the system PTE increases gradually and the output power of receiver 1 decreases slightly. It should be mentioned that the underwater WPT system can deliver about 200 W of power with a 92.25% PTE under four loads.

It is inevitable that the magnetic coupler will be offset when the AUV enters the docking station for charging. Taking the mechanical capture and clamping mechanism in the docking station into consideration, PTE and output power are measured in the range of 20 mm lateral misalignment, 20 mm axial misalignment, and 10° rotational misalignment. A schematic of the above three offset cases of the magnetic coupler is shown in Fig. 8. The experimental results are plotted in Fig. 9. In the misalignment process, PTEs remain relatively stable, and the maximum fluctuation rate of output power is 9.7%. The results show that the designed magnetic coupler has excellent tolerance ability for misalignment.

The performance of the data transfer link during wireless charging is studied. Fig. 10 depicts the experimental waveforms of U_{s}, U_{dt}, U_{dr}, and U_{o} at a data rate of 30 kbps. It can be observed that origin data has been correctly transmitted and

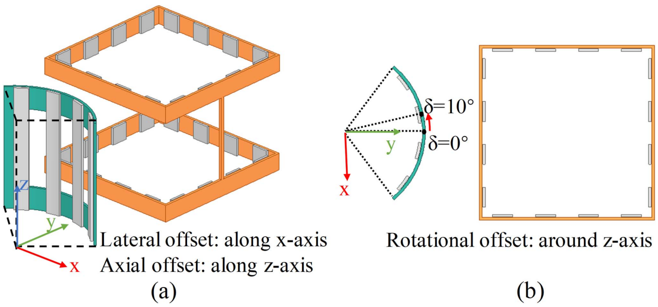

Fig. 8. Illustration of different misalignment types of the magnetic coupler. (a) Lateral and axial misalignment. (b) Rotational misalignment.

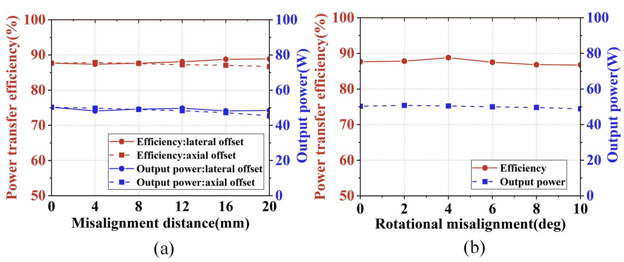

Fig. 9. PTE and output power variations under different misalignment types. (a) Lateral and axial misalignment. (b) Rotational misalignment.

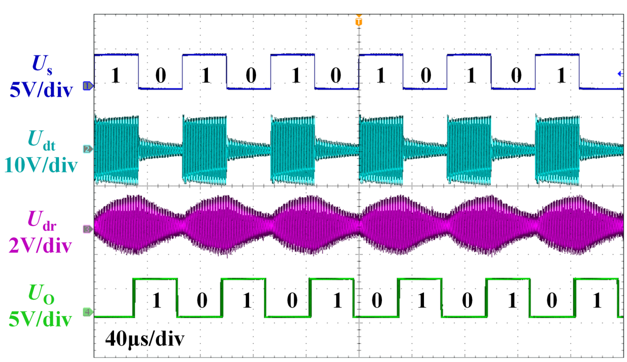

Fig. 10. Experimental waveforms of data transfer link.

demodulated. The feasibility of the proposed SWPDT scheme has been demonstrated. In addition, the data transfer delay is 30 μs via the coupling link, modulation, and demodulation module.

V. Conclusion

A SWPDT system based on a multidirectional magnetic coupler is proposed for swarm AUVs. By employing NSGA-II, the parameters of the magnetic coupler are optimized to achieve a tradeoff between mutual inductance and core volume. Also, a hybrid injection communication method based on the *LCC-S* compensation topology is designed and analyzed. The results indicate that the system can reach the PTE of 92.25% with four loads when the total output power is 200 W. And it has better offset insensitive properties. Moreover, the data rate of the SWPDT system is 30 kpbs at a 5 cm distance under seawater.

References

[1] C. Can, S. Wu, Z. Zhang, L. Jiang, and S. Yang, "Development of a fit-to-surface and lightweight magnetic coupler for autonomous underwater vehicle wireless charging systems," *IEEE Trans. Power Electron.*, vol. 36, no. 9, pp. 9927–9940, Sep. 2021.

[2] L. Yang, M. Ju, and B. Zhang, "Bidirectional undersea capacitive wireless power transfer system," *IEEE Access*, vol. 7, pp. 121046–121054, Aug. 2019.

[3] F. Lu et al., "A high-efficiency and long-distance power-relay system with equal power distribution," *IEEE J. Emerg. Sel. Topics Power Electron.*, vol. 8, no. 2, pp. 1419–1427, Jun. 2020.

[4] C. Lu et al., "Design and analysis of an omnidirectional dual-band wireless power transfer system," *IEEE Trans. Antennas Propag.*, vol. 69, no. 6, pp. 3493–3502, Jun. 2021.

[5] L. Tan et al., "Power stability optimization design of three-dimensional wireless power transmission system in multi-load application scenarios," *IEEE Access*, vol. 8, pp. 91843–91845, May 2020.

[6] N. Ha-Van, Y. Liu, P. Jayathurathnage, C. R. Simovski, and S. A. Tretyakov, "Cylindrical transmitting coil for two-dimensional omnidirectional wireless power transfer," *IEEE Trans. Ind. Electron.*, vol. 69, no. 10, pp. 10045–10054, Oct. 2022.

[7] Z. Yan, K. Zhang, L. Qiao, Y. Hu, and B. Song, "A multi-load wireless power transfer system with concentrated magnetic field for AUV cluster system," *IEEE Trans. Ind. Appl.*, vol. 58, no. 1, pp. 1307–1314, Jan./Feb. 2022.

[8] L. Yang et al., "Undersea wireless power and data transfer system with shared channel powered by marine renewable energy system," *IEEE J. Emerg. Sel. Topics Circuits Syst.*, vol. 12, no. 1, pp. 242–250, Mar. 2022.

[9] G. Chen et al., "Wireless power and data transmission system of submarine cable-inspecting robot fish and its time-sharing multiplexing method," *Electronics*, vol. 8, no. 8, Jul. 2019, Art. no. 838.

[10] J. Wu, C. Zhao, Z. Lin, J. Du, Y. Hu, and X. He, "Wireless power and data transfer via a common inductive link using frequency division multiplexing," *IEEE Trans. Ind. Electron.*, vol. 62, no. 12, pp. 7810–7820, Dec. 2015.

[11] J. Wu et al., "A simultaneous wireless information and power transfer system with independent channel for information transfer," *IEEE Access*, vol. 8, pp. 125610–125619, Jul. 2020.

[12] G. Wei, J. Feng, J. Zhang, C. Wang, C. Zhu, and S. Y. Ostanin, "An efficient power and data synchronous transfer method for wireless power transfer system using double-D coupling coil," *IEEE Trans. Ind. Electron.*, vol. 68, no. 11, pp. 10643–10653, Nov. 2021.

[13] H. Cha, K. Park, T. Kim, and R.-Y. Kim, "Design of magnetic structure for omnidirectional wireless power transfer," *IEEE Trans. Power Electron.*, vol. 36, no. 8, pp. 8849–8860, Aug. 2021.

[14] Z. Luo, X. Wei, M. G. S. Pearce, and G. A. Covic, "Multiobjective optimization of inductive power transfer double-D pads for electric vehicles," *IEEE Trans. Power Electron.*, vol. 36, no. 5, pp. 5135–5146, May 2021.

[15] F. Wen, X. Chu, Q. Li, R. Li, L. Liu, and F. Jing, "Optimization on three-coil long-range and dimension-asymmetric wireless power transfer system," *IEEE Trans. Electromagn. Compat.*, vol. 62, no. 5, pp. 1859–1868, Oct. 2020.